

## Original Article

# Nasal Structural and Aerodynamic Features That May Benefit Normal Olfactory Sensitivity

Chengyu Li<sup>1</sup>, Jianbo Jiang<sup>1</sup>, Kanghyun Kim<sup>1,2</sup>, Bradley A. Otto<sup>1</sup>, Alexander A. Farag<sup>1</sup>, Beverly J. Cowart<sup>3,4</sup>, Edmund A. Pribitkin<sup>4</sup>, Pamela Dalton<sup>3</sup> and Kai Zhao<sup>1,2</sup>

<sup>1</sup>Department of Otolaryngology—Head & Neck Surgery, The Ohio State University, Columbus, OH 43212, USA,

<sup>2</sup>Department of Biomedical Engineering, The Ohio State University, Columbus, OH 43211, USA <sup>3</sup>Monell Chemical Senses Center, Philadelphia, PA 19104, USA and <sup>4</sup>Department of Otolaryngology—Head & Neck Surgery, Thomas Jefferson University, Philadelphia, PA 19107, USA

Correspondence to be sent to: Kai Zhao, Department of Otolaryngology—Head & Neck Surgery, The Ohio State University, Columbus, OH 43212, USA. e-mail: [kai.zhao@osumc.edu](mailto:kai.zhao@osumc.edu); [zhao.1949@osu.edu](mailto:zhao.1949@osu.edu)

Editorial Decision 12 February 2018.

## Abstract

Nasal airflow that effectively transports ambient odors to the olfactory receptors is important for human olfaction. Yet, the impact of nasal anatomical variations on airflow pattern and olfactory function is not fully understood. In this study, 22 healthy volunteers were recruited and underwent computed tomographic scans for computational simulations of nasal airflow patterns. Unilateral odor detection thresholds (ODT) to l-carvone, phenylethyl alcohol (PEA) and d-limonene were also obtained for all participants. Significant normative variations in both nasal anatomy and aerodynamics were found. The most prominent was the formation of an anterior dorsal airflow vortex in some but not all subjects, with the vortex size being significantly correlated with ODT of l-carvone ( $r = 0.31$ ,  $P < 0.05$ ). The formation of the vortex is likely the result of anterior nasal morphology, with the vortex size varying significantly with the nasal index (ratio of the width and height of external nose,  $r = -0.59$ ,  $P < 0.001$ ) and nasal vestibule “notch” index ( $r = 0.76$ ,  $P < 0.001$ ). The “notch” is a narrowing of the upper nasal vestibule cartilage region. The degree of the notch also significantly correlates with ODT for PEA ( $r = 0.32$ ,  $P < 0.05$ ) and l-carvone ( $r = 0.33$ ,  $P < 0.05$ ). ODT of d-limonene, a low mucosal soluble odor, does not correlate with any of the anatomical or aerodynamic variables. The current study revealed that nasal anatomy and aerodynamics might have a significant impact on normal olfactory sensitivity, with greater airflow vortex and a narrower vestibule region likely intensifying the airflow vortex toward the olfactory region and resulting in greater olfactory sensitivity to high mucosal soluble odors.

**Key words:** computational fluid dynamics, medical image-based modeling, nasal airflow vortex, nasal valve notch

## Introduction

Nasal airflow that effectively transports ambient airborne odorants to the olfactory receptors located in the superior region of the nasal cavity is a critical prerequisite for normal human olfactory function. It is well established that human olfactory acuity has significant variability, with much research focused on receptor genetics and

postreceptor neural variations among subjects (Ignatieva et al. 2014; Mainland et al. 2014). However, to date, the degree of variation in olfactory acuity that can be accounted for by differences in internal nasal anatomy and aerodynamics has not been addressed.

During a normal breath, less than 15% of the air inhaled flows through the olfactory region (Stuiver 1958; Hahn et al. 1993;

Keyhani et al. 1995; Subramaniam et al. 1998; Kelly et al. 2000), and significant normative variations in both nasal anatomy and aerodynamics have been reported. The most prominent is the formation of an airflow vortex in the anterior dorsal region in some but not all subjects (Keyhani et al. 1997), with the intensity of the vortex recently reported to correlate significantly with the nasal index (Zhao and Jiang 2014). Yet, direct associations between such aerodynamic variations and olfactory acuity have never been established, although studies of regional variation in nasal volume from computed tomographic (CT) scans have provided support for the notion that local volume changes in nasal airway may affect olfactory function (Leopold 1988; Damm et al. 2002). Our previous study using a three-dimensional anatomically accurate nasal cavity model based on one individual's CT scan (Zhao et al. 2004) also confirmed that, depending on the location, relatively minor changes in critical nasal regions may dramatically alter airflow distribution and greatly affect the ability of odorant molecules to access the olfactory epithelium. However, these were only theoretical calculations without human testing to confirm it.

Historically, nasal anatomical variations have been reported as the nasal index, which is the ratio of the external nasal width and height. Ecogeographic variation in nasal index has been posed as an example of human morphological adaptation to climate, with broad noses (platyrrhine) evolving in habitats with warm, humid environments and narrow noses (leptorrhine) evolving in colder climates where the air needs more warming (Thomson and Buxton 1923; Zaidi et al. 2017). Zhao and Jiang (2014) have shown that these anterior nasal structure variations may also have an impact on airflow patterns, with narrower and taller external noses more likely to form intense anterior dorsal vortices. Ramprasad and Frank-Ito (2016) reported distinct anatomical variations in the nasal vestibule (they termed it “notch”) in another sample of healthy controls that may result in regional variations of aerodynamic resistance, although it is unclear whether the notch is related to the nasal index. The functional relevance of these anatomical and aerodynamic variations and their potential impact on olfactory function have not been investigated.

The understanding of normative peripheral mechanisms of olfactory function variability may have broad implications, for example, on the design human olfactory psychophysical tests and selection sensory panels in the flavor and fragrance industry, as well as in the clinical field, where nasal obstruction associated with nasal sinus disease is a prevalent cause of olfactory dysfunction (Zhao et al. 2014). Yet, the association of nasal obstruction with olfactory loss cannot be fully understood without the knowledge of the impact of nasal anatomy and its variation among healthy subjects. The currently available objective measures of nasal airflow (i.e., acoustic rhinometry or rhinomanometry) are capable of indexing only global airflow or static airway dimensions, and they correlate poorly with patients' subjective symptoms.

Computational fluid dynamic (CFD) modeling techniques (Keyhani et al. 1995; Subramaniam et al. 1998; Zhao et al. 2004; Zhao, Dalton, et al. 2006; Zhao, Pribitkin, et al. 2006; Shen, Hur, Li, et al. 2017; Shen, Hur, Zhao, et al. 2017) have been used to quantify anatomical-dependent changes in nasal airflow pattern. Thus, the goal of this project was to characterize the functional impact of nasal aerodynamic variations on human olfaction with CFD approaches. In the future, CFD models can be established as a viable technique for predicting or optimizing the functional impact of nasal airway anatomy and nasal airflow on olfaction, and potentially for identifying the nasal structural features that need to be preserved in surgery for optimal olfactory outcomes.

## Materials and methods

### Human subjects

This study presents additional data from a previously published study (Zhao and Jiang 2014), where 22 healthy subjects underwent CT scans for CFD modeling. The group consisted of 10 males and 12 females: 20 Caucasian, 1 African American, and 1 Asian American. Their ages ranged from 21 to 39 years, with a mean of 25.6, median of 24.5, and standard deviation (SD) of 4.84 years. The study was approved by the University of Pennsylvania and Thomas Jefferson University institutional review boards. Written informed consent was obtained from all volunteers. All of the participants underwent medical history screening to exclude pre-existing nasal sinus disease, severe seasonal or perennial allergies, prior olfactory complaint, head trauma, and prior nasal surgery. Both acoustic rhinometry and rhinomanometry were performed immediately before the CT scan on all subjects to objectively confirm the absence of severe nasal obstruction. Genetic diversity in functioning olfactory receptors has been reported between African Americans and non-African Americans (Menashe et al. 2003), but in this small sample, subject enrollment was predominantly Caucasian.

### Unilateral odor detection thresholds

Within the same visit, unilateral olfactory thresholds for three commonly encountered odorants (l-carvone [minty], phenylethyl alcohol [PEA, rose-like], and d-Limonene [orange-like]) were obtained for all participants. These odorants were selected due to their distinct sorptive properties in nasal mucus: d-limonene is quite insoluble, whereas PEA and l-carvone are highly soluble, although experimental data in mucus only exists for l-carvone (Hornung et al. 1987). Animal studies have demonstrated that as airflow rate decreases, neural responses to more sorptive odors are more affected (diminished) than those to less sorptive odors (Scott et al. 2014). A similar effect in humans was reported, where the perceived intensity of an odorant classified as more sorptive (l-carvone) was lower when perceived through the nostril with the lower nasal-cycle flow rate relative to the higher flow rate nostril (Sobel et al. 1999). On the basis of this evidence, we hypothesized that sensitivity to highly soluble odorants (PEA and l-carvone) would be more affected by variations in nasal anatomic and aerodynamic features than would sensitivity to the less soluble d-limonene.

Thresholds for all three odorants were determined through a two-alternative, forced-choice, stair-case method that has been previously described in detail (Wetherill and Levitt 1965; Pribitkin et al. 2003). Each odorant series consisted of 24 bottles of differing concentrations, beginning with a neat solution (step 0) and extending in half-log (for PEA) or binary (for l-Carvone and d-Limonene) dilution steps in glycerol for 23 steps. The head space airborne odorant concentration for each dilution sample was calibrated and measured using gas chromatography (Zhao et al. 2014). The threshold was measured in one nostril while the other was blocked by a foam plug, then was repeated in the other nostril, in a counter-balanced order.

### Nasal index

The nasal index was determined as the ratio of the external nasal width and height based on CT-reconstructed facial features, as illustrated in Figure 1. There has been some interest in the rhinology field in predicting nasal physiology and its susceptibility to nasal sinus disease by easily obtainable external physical measurements. However, no correlation between the nasal index and nasal resistance has been found (Leong et al. 2010; Doddi and Eccles 2011). Here, we examined the relationship between nasal index and olfactory sensitivity.

**Rhinometry measurement**

The unilaterally minimum (narrowest) cross-sectional area (MCA) in the anterior 5 cm of the nasal airway was determined for each subject using acoustic rhinometry (SRE21000, RhinoMetrics A/S). Nasal resistance (Clement 1984) during normal breathing was measured unilaterally by anterior rhinomanometry (SRE21000, RhinoMetrics A/S) at reference pressure drop of 75 Pa.

**CFD modeling**

Three-dimensional numerical nasal models that are suitable for numerical simulation of nasal airflow and odorant transport were

constructed based on each participant's CT scans, as shown in Figure 2. The details of the method can be found in our previous publications (Zhao et al. 2004; Li, Farag, Maza, et al. 2017; Li, Jiang, et al. 2017; Otto et al. 2017; Lee et al. 2018). In brief, the interface between the nasal mucosa and the air was delineated on the scans (using AMIRA, Visualization Sciences Group). Then, the nasal cavity air space was filled with tetrahedral elements (using ICEM CFD, ANSYS Inc.). A thin (~0.2 mm) region consisting of four layers of compact hybrid tetrahedral/pentahedral elements was created near the mucosal surface to more accurately model the rapidly changing near-wall air velocity and odorant concentration. To achieve grid

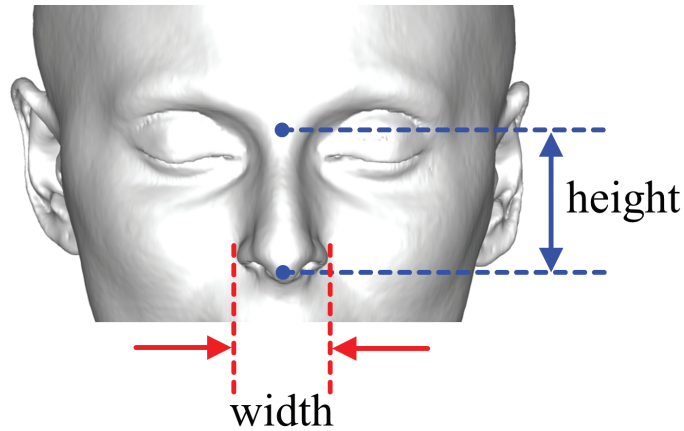


Figure 1. Facial reconstruction based on CT scan, and measurement of nasal index as the ratio of external nasal width and height.

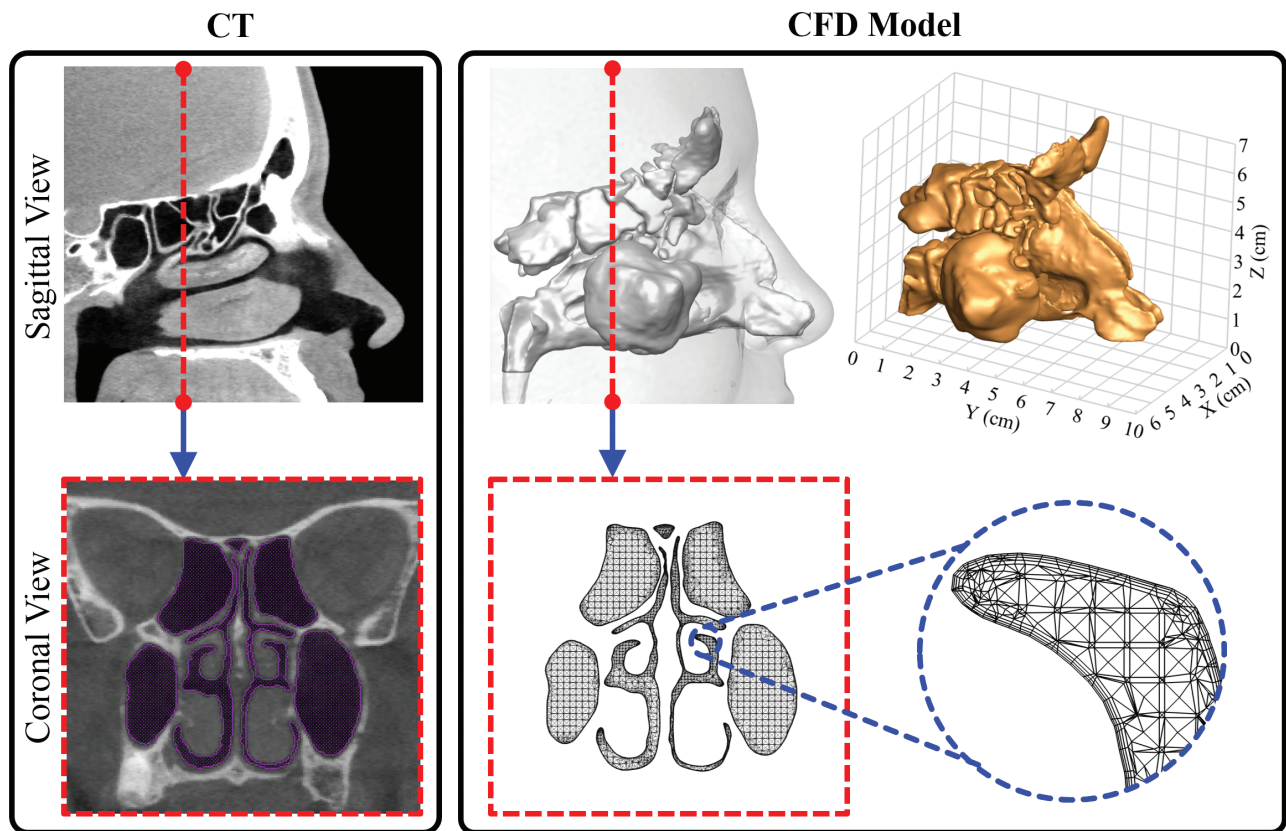


Figure 2. CT-based computational model. Side-by-side comparison of the CT scan and CFD model from sagittal and coronal views, respectively. The dashed line indicates the slice cut on the sagittal plane. The perspective view of the 3D model and its dimensions are shown on the right top plot. In a close-up view (right bottom), layers of small and fine elements along the wall can be seen; these capture the rapid near wall changes of air velocity and odorant concentration and are essential for accurate numerical simulations.

independent solutions, the computational meshes were refined by gradient adaptation and boundary adaptation protocols as previously described (Zhao et al. 2004; Li, Farag, Leach, et al. 2017; Li, Jiang, et al. 2017; Otto et al. 2017). As a result, the final grid consisted of ~1.8–3.5 million elements. Next, inspiratory quasi-steady laminar (Keyhani et al. 1995; Zhao et al. 2004) and turbulent nasal airflow (Zhao, Dalton, et al. 2006) were simulated (Fluent, ANSYS Inc.) by applying physiologically realistic pressure drops between the nostrils and the nasal pharynx. A pressure drop of 15 Pa is prescribed for restful breathing (Zhao et al. 2004) and 150 Pa for sniffing (Zhao, Dalton, et al. 2006). The averaged inspiratory flow rate under 15 Pa among our cohort was  $14.5 \pm 4.2$  L/min, close to the typical range of 15 L/min for restful breathing. The low-Reynolds-number  $k-\omega$  turbulence model was used to simulate the flow field with a turbulence intensity of 2.5% (Hahn et al. 1993) of the mean velocity imposed at inlet location and compared with the laminar model to investigate possible turbulence effects. The low-Reynolds-number  $k-\omega$  turbulent model has been shown to be valid and reliable in the prediction of laminar, transitional, and turbulent flow behavior (Wilcox 2006). Along the nasal walls, the no-slip boundary condition was applied, and the wall is assumed to be rigid. At the nasopharynx, the “pressure outlet” condition was adopted.

The numerical solutions of the continuity, momentum, and/or turbulence transport equations were determined using the finite-volume method. A second-order upwind scheme was used for spatial discretization. The SIMPLEC algorithm was used to link pressure and velocity. The discretized equations were then solved sequentially using a segregated solver. Convergence was obtained when the scaled residuals of continuity, momentum, and/or turbulence quantities were  $<10^{-5}$ . Global quantities such as flow rate and pressure on the nasal walls were further monitored to check the convergence.

### Data analysis

Prior to data analysis, CFD models of each subject were validated by comparison of cross-sectional cuts with corresponding CT images to ensure the anatomical accuracy of the model. Then, nasal airflow patterns for each subject were simulated and visually inspected. Pearson correlations between each of these independent variables and the dependent variables, odor detection threshold (ODT), were

examined. The correlations between the variables were performed unilaterally, which differs from the previously published bilateral analyses (Zhao and Jiang 2014). All analyses were carried out in IBM SPSS Statistics 22.0 (IBM Corp.).

## Results

### Nasal geometries and airflow patterns

Flow patterns inside the nasal cavity of each subject were characterized and visualized with airflow streamline, generated with neutral-buoyant tracking particles uniformly released on the nostril plane. To visualize airflow streamlines, 300 tracking seeds were uniformly released for each subject and for each side of nostril. While several features of the streamline patterns were found to vary across the subjects, the most prominent variation was the formation of an anterior dorsal vortex, right after the nasal valve, which was found in some subjects but not in others. To quantify the size of the vortex, a vortex index is defined as the maximum vortex length ( $D$ ) normalized by the nasal cavity length ( $L$ ) for each subject, as shown in Figure 3a (Vortex Index =  $D/L$ ). We further categorized the vortex index as significant vortex (vortex index  $> 20\%$ ), small vortex ( $0\% < \text{vortex index} < 20\%$ ), and no vortex (vortex index =  $0\%$ ), as shown in Figure 5. These categories were only used to facilitate better description and sample selection for figure plotting. In the correlation analyses below, it was the continuous vortex index that was used, not the categories. The formation of this anterior dorsal vortex has been reported in a few previous studies (Swift and Proctor 1977; Zhao and Jiang 2014), and may be due to the narrowing of the nasal valve and abrupt volume increase downstream. The distribution of unilateral vortex indices (significant vortex,  $n = 13$ ; small vortex,  $n = 10$ ; no vortex,  $n = 21$ ) confirmed that this vortex is quite common among healthy cohort. A significant correlation (Table 1) was found between the vortex index and nasal index ( $r = -0.59$ ,  $P < 0.001$ ), indicating that a narrower anterior nasal morphology may result in a more intense airflow vortex.

Another nasal anatomical feature—partial narrowing of the superior nasal valve, termed “notch”—has been recently reported (Ramprasad and Frank-Ito 2016), and we hypothesized that it might promote vortex formation at the anterior dorsal airspace.

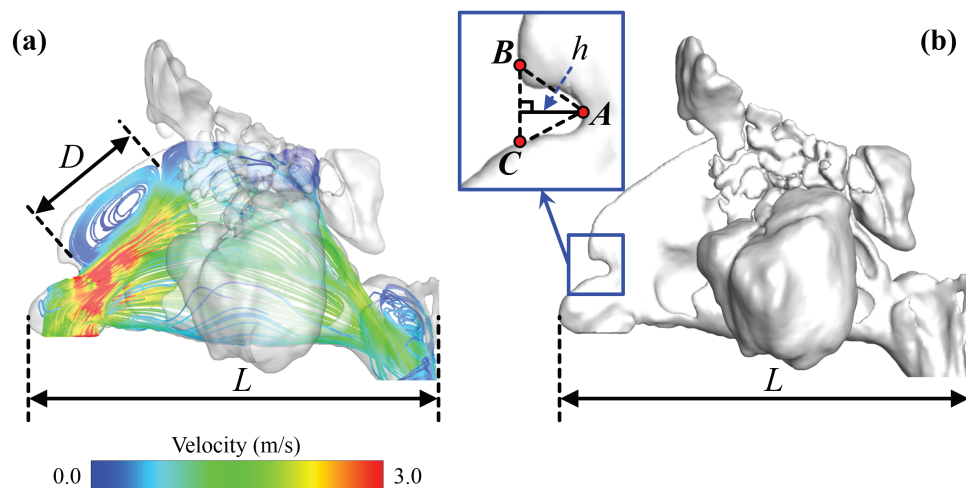


**Figure 3.** Measurements of vortex index (a) and notch index (b). The vortex index is defined as the ratio of vortex length ( $D$ ) and nasal cavity length ( $L$ ). The notch index is defined as the ratio of notch depth ( $h$ ) and nasal cavity length ( $L$ ). In plot (b), point A indicates the deepest point of the nasal notch. The line BC is the extension line along the tangential direction of the anterior dorsal curve. The notch depth ( $h$ ) is defined as the perpendicular distance from point A to line BC.

To quantify the size of the nasal notch, we first defined the deepest point of the notch (point A in Figure 3b), then drew the tangential line along the curvature of the anterior dorsal geometry (line BC in Figure 3b). The notch depth ( $b$ ) was measured as the perpendicular distance from point A to line BC. A notch index was determined as the ratio of notch depth and nasal cavity length (notch index =  $b/L$ ). We further categorized the degree of the notch as significant notch (notch index > 5%), small notch (0% < notch index < 5%), and no notch (notch index = 0%). Figure 4 shows examples of subjects with (a) a significant notch, (b) a small notch, and (c) no notch in endoscopic view simulated by the software ParaView 5.1.2 (Kitware Inc.) based on CT scans. The distribution of unilateral notch indices (significant notch,  $n = 13$ ; small notch,  $n = 13$ ; no notch,  $n = 18$ ) confirmed that a notched nasal phenotype is quite common in this population—59% of subjects have different levels of notch (notch index > 0%). Again, these categories were only used to facilitate better description and sample selection for figure plotting. In all the data analyses below, it was the continuous notch index that was used, not the categories. A significant correlation was found between notch and vortex indices ( $r = 0.76$ ,  $P < 0.001$ ), indicating that subjects with pronounced “notches” were more likely to form an airflow vortex. As shown in Figure 5, 85% of subjects with a significant notch also formed a significant anterior dorsal vortex in the nasal cavity, and 89% of subjects who did not possess a notch did not show any vortex formation.

The average nasal index in our sample (range from 0.59 to 0.87, with a mean of 0.71, median of 0.72, and SD of 0.08) was indicative of a leptorrhine nose (tall and narrow), which is consistent with the majority Caucasian composition of our subjects (Leong and Eccles 2009). A significant correlation was found between nasal index and

notch index ( $r = -0.56$ ,  $P < 0.001$ , see Table 1). As illustrated in Figure 6, it also appears that a narrower and taller external nose is more likely to have a pronounced notch, which may in turn lead to flow separation and formation of the vortex. Furthermore, the experimentally measured MCA significantly correlated with nasal index ( $r = 0.56$ ,  $P < 0.001$ ), notch index ( $r = -0.54$ ,  $P < 0.001$ ), and vortex index ( $r = -0.47$ ,  $P = 0.001$ ). However, nasal resistance showed no significant correlations with any of those measures.

To address the concern of treating the notch and vortex indices from each side of the nose as independent variables, we examined the correlations between the left and right sides of the same patients and found no significant correlation, as shown in Figure 7, reflecting significant unilateral differences. Among the 22 healthy subjects tested, 59.1% of total subjects had different notch categories between the two sides, and 31.8% had different vortex categories. With the exception of the nasal index, all variables collected in the study were unilateral. Thus, to potentially capture any unilateral differences as well as in consideration of the fact that two sides of the nose are parallel passages—that aerodynamics features on one side should not substantially affect the other—all data analyses were carried out unilaterally, with the same nasal index value assigned to both sides.

### Impacts on olfactory function

We further examined the relationship between each of these anatomical and aerodynamic variables and the dependent variables of measured ODT among the subjects. Significant correlations were found between ODT of *L*-Carvone and both vortex index ( $r = 0.31$ ,  $P = 0.0498$ ) and notch index ( $r = 0.33$ ,  $P = 0.032$ ). Significant correlation was also found between ODT of PEA and the notch index

**Table 1.** Pearson correlation matrix between variables ( $n = 44$ )

	MCA	Nasal index	Notch index	Vortex index	ODT PEA	ODT <i>D</i> -Limonene	ODT <i>L</i> -Carvone
Nasal resistance							
MCA		0.56**	-0.54**	-0.47**			
Nasal index			-0.56**	-0.59**			
Notch index				0.76**	0.32*		0.33*
Vortex index							0.31*
ODT PEA						0.46**	
ODT <i>D</i> -Limonene							0.31*
ODT <i>L</i> -Carvone							

\* $P < 0.05$ . \*\* $P < 0.01$ .

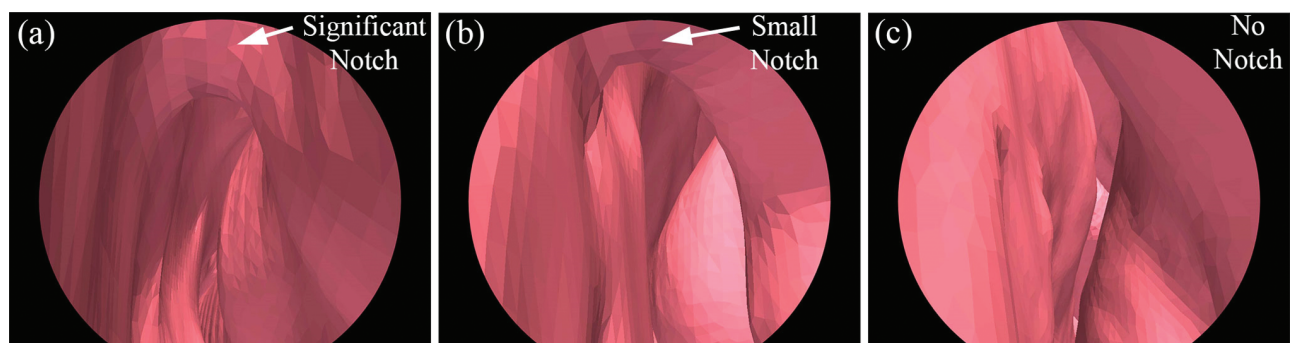


**Figure 4.** Endoscopic view of the nasal valve region of a significant (a), a small (b), and an absence of notch (c). The views are generated by ParaView 5.1.2 (Kitware Inc.) based on CT scans.

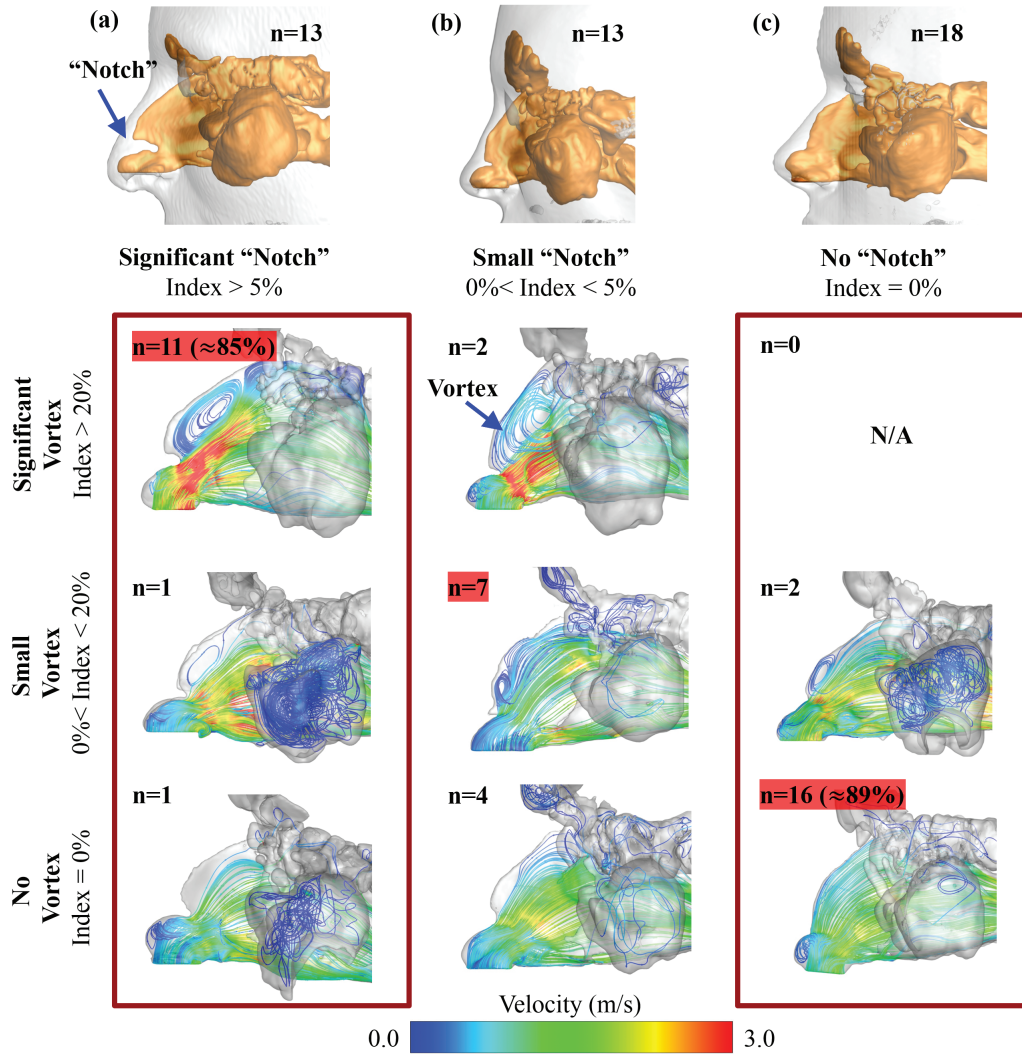


**Figure 5.** Sagittal view showing external nose (gray transparent) and morphology of the nasal vestibule airway (gold solid) for each phenotype. (a) significant notch (notch index > 5%). (b) small notch (notch index < 5%). (c) no notch (notch index = 0%). The "n" values indicate the number of sides that were categorized into each phenotype. Airflow streamline patterns in the nasal cavity were categorized based on the formation of anterior–superior airflow vortex. Depending on its nasal notch index (=0%; <5%; >5%) and vortex index (=0%; <20%; >20%), unilateral nasal cavities were categorized into nine different types. The "n" values indicate the number of sides of all subjects that were categorized into each type.

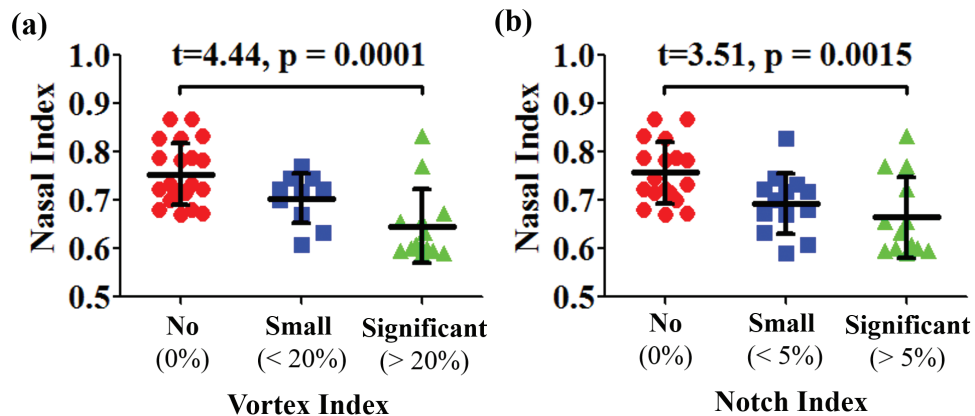


**Figure 6.** Nasal index distribution for all subjects with various scores of the vortex index (a) and notch index (b). The nasal index for the subjects with significant vortex (vortex index > 20%) was significantly lower than that of the subjects with no vortex (vortex index = 0%) in their nasal airflow. Similarly, the nasal index for the subjects with significant notch (notch index > 5%) was significantly lower than that of the subjects with no notch (notch index = 0%) for their nasal anatomy.

( $r = 0.32$ ,  $P = 0.034$ ). However, ODT of *D*-Limonene, a lower mucosal soluble odor, did not correlate with either notch index or vortex index.

As shown in Figure 8a–c, subjects with a significant notch (notch index > 5%) had significantly better olfactory detection thresholds for *L*-Carvone ( $P = 0.021$ ) and for PEA ( $P = 0.04$ ) than did those with no notch, but not for *D*-Limonene. Similarly, if we group the subjects according to the vortex index, Figure 8d–f illustrates that subjects with a significant vortex (vortex index > 20%) have better olfactory detection thresholds for *L*-Carvone ( $P = 0.023$ ) and PEA ( $P = 0.054$ , strong tendency), but not for that of *D*-Limonene than do subjects with no vortex. These findings indicate that a higher notch index (greater narrowing in the nasal vestibule regions) and higher vortex index (more intense superior airflow vortex) may result in better olfactory sensitivity. ODT of *D*-Limonene, a low mucosal soluble odor, does not correlate with any of the anatomical or aerodynamic

variables, even though ODTs of PEA, *L*-Carvone, and *D*-Limonene correlated significantly with each other, as expected (Zhao et al. 2014). No significant correlation was found between nasal resistance, nasal index, or MCA and any of the olfactory thresholds.

The above analyses were repeated for higher inspiratory flow rate at 150 Pa by applying the low-Reynolds-number  $k-\omega$  turbulence model, and the results were consistent with those found with restful breathing flow rates. Analyses were also repeated excluding the two non-Caucasian subjects, and no substantial changes in findings were observed.

## Discussion

Normative variations in anatomical features of the nasal airway have been widely reported in the past. The nasal index (width/height) is known to show significant racial variation (Thomson and Buxton 1923).

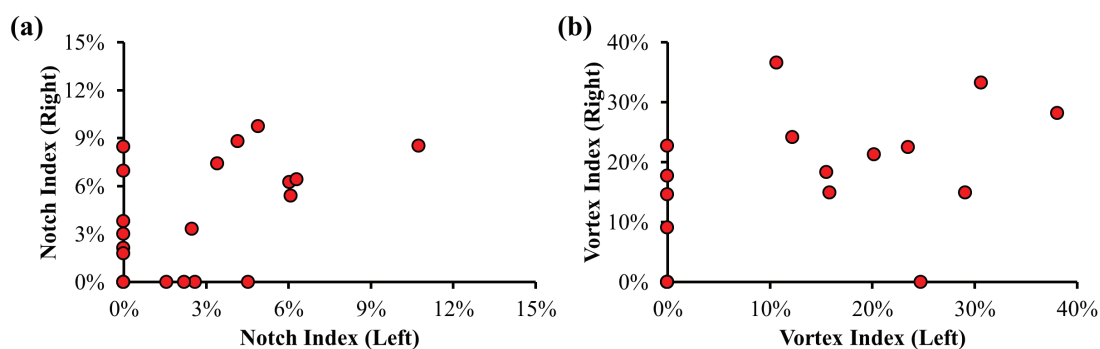


**Figure 7.** Scatter diagram of the notch index (a) and vortex index (b) between left and right side of the same subjects. Among 22 tested healthy controls, there was no significant correlation between left and right side of the nose for either the notch index or the vortex index.

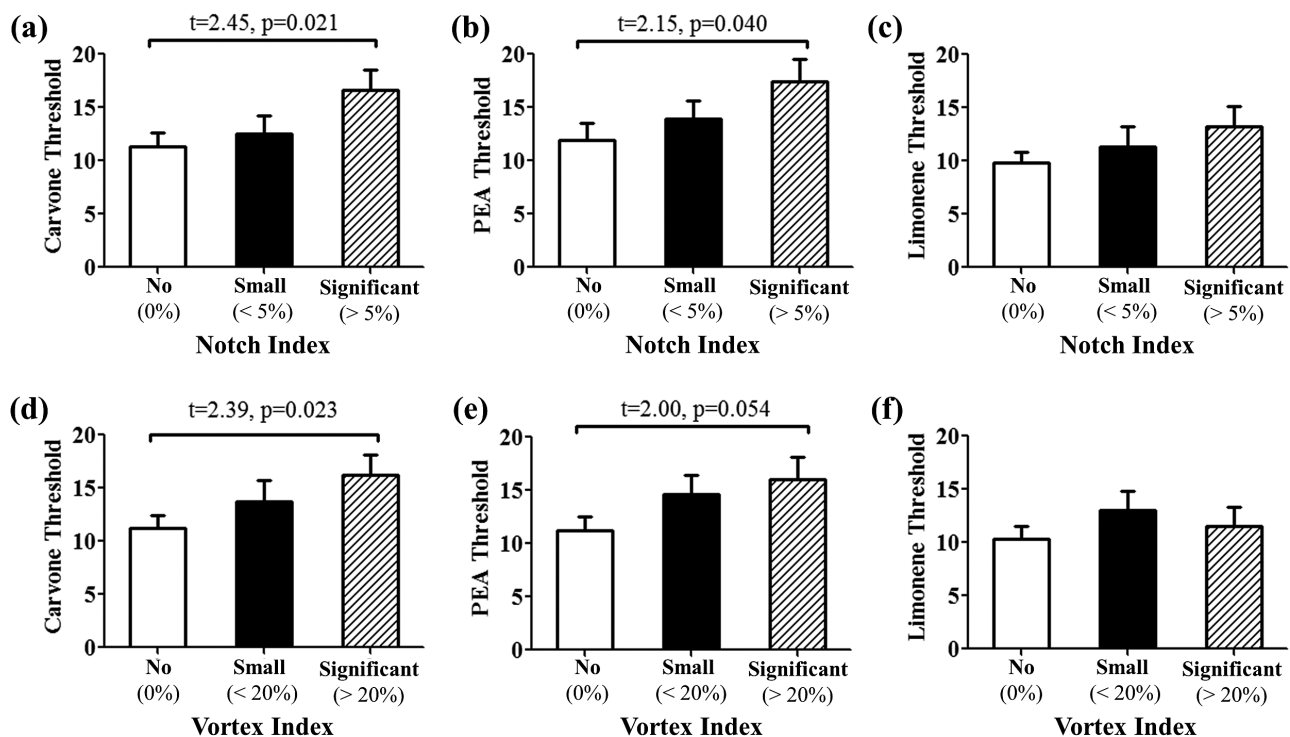


**Figure 8.** ODT for *L*-Carvone (a, d), PEA (b, e), and *D*-Limonene (c, f). Subjects with significant nasal valve notch (notch index > 5%) and more intense anterior airflow vortex (vortex index > 20%) are likely to have better olfactory sensitivity to an odorant with high mucosal solubility (*L*-Carvone and PEA), but not an odorant with low mucosal solubility (*D*-Limonene).

A typical Caucasian nose has a nasal index <0.70. A nasal index between 0.70 and 0.85 is described as mesorhine. A platyrrhine nose has a nasal index greater than 0.85. The difference in nasal index among populations may be the result of adaptations to climate, evolutionary factors, or simply genetic drift (Zaidi et al. 2017). In addition, distinct internal nasal vestibule structures (“notch”) were also found within a small sample of human noses (Ramprasad and Frank-Ito 2016). In our current study, we further quantified the degree of the nasal notch and found it significantly correlated with the nasal index ( $r = -0.56$ ,  $P < 0.001$ ). This negative correlation indicates that a narrow nose is more likely to present with a notch in the nasal valve region than is a broad nose. In addition, both the nasal index and notch index were found to correlate significantly with nasal MCA ( $r = 0.56$ ,  $P < 0.001$ ;  $r = -0.54$ ,  $P < 0.001$ ). However, neither the nasal index nor the notch index correlated significantly with nasal resistance, which replicates previous findings in the literature (Leong and Eccles 2009; Doddi and Eccles 2011).

Normative variations in the aerodynamic features of the nasal airway have also been implicated in the past. The formation of an anterior–superior airflow vortex was first reported by Swift and Proctor (1977) in a case report of one healthy subject. On the basis of simulation in one subject, Keyhani et al. (1997) speculated that the formation of such an airflow vortex may be due to narrowing of the nasal valve and an abrupt volume increase after the nasal valve. Zhao and Jiang (2014) confirmed that such airflow variations are widely present in healthy subjects. The current study provides the first connection between these aerodynamic and anatomical features: a strong correlation between lower nasal index, lower MCA, higher “notch,” and the more likely formation of the anterior–superior airflow vortex. The abrupt volume changes before and after the “notch” could induce airflow recirculation—hence the vortex. Consequently, the majority (85%) of nasal airways with a significant nasal “notch” appear to have an airflow vortex ipsilaterally (Figure 5).

However, there is a continuing debate on the functional relevance of these internal nasal anatomy variations and their associated airflow patterns within a healthy population. Some have suggested these are simply the result of genetic drift (Spitze 1993; Whitlock and Guillaume 2009). It is well recognized that human olfactory acuity has significant variability within a normal population, with much research focused on receptor genetics and postreceptor neural variations (DeMaria et al. 2013; Mainland et al. 2014). It has also been hypothesized that nasal anatomical and aerodynamic variations may potentially benefit olfactory sensitivity (Zhao and Dalton 2007). The current study provides the first direct evidence of the potential impact of normal variation in nasal structure and aerodynamics on normative variations in olfactory sensitivity. It suggests that a “notch” in the nasal vestibule region may improve olfactory sensitivity to some odorants, potentially due to the formation of an airflow vortex in the nasal valve region. The airflow vortex may promote odor plume mixing, increase its resident time within the olfactory region, and benefit odorants with high mucosal solubility. In contrast, sorption of less soluble odorants, as was reported previously (Scott et al. 2014), seems to be only limited physically by their low solubility and not affected by increased flow rate or resident time. This finding may have broad implications. Variations contributed by differences in internal nasal anatomy and aerodynamics may need to be accounted for, for example, in screening for subjects when investigating olfactory function, or screening for sensory panels in flavor and fragrance research depending on the solubility profiles of the flavors and fragrances. It also remains to be investigated whether

the anatomical and aerodynamic variations would make a subset of the population more susceptible to obstruction-related olfactory losses or damage from inhaled toxins.

The lessons learned here may also be applicable to bio-inspired artificial noses. Aerodynamics is central to olfaction because it plays a vital role in odor sampling. To provide the best opportunity for odorant molecules to contact the sensory epithelium, an artificial olfaction device could either increase sensor surface area or increase the odorant resident time within a limited nasal volume. Creating an airflow recirculation may benefit detection by increasing odorant resident time, especially for odorants with high solubility.

### Limitations and future work

The current study is limited by its predominantly Caucasian cohort (20/22). Starting a new area of research with a simple racial composition is often necessary given small sample sizes, before expanding to a more diverse racial composition. It is possible that the “notch” is a common feature across more diverse demographics, as the previous study (Ramprasad and Frank-Ito 2016) reporting the “notch” involved 16 subjects from four different ethnic groups—African American (Black), Asian, Caucasian, and Latin American—although the exact numbers for each group were not provided. Thus, our study needs to be replicated with a larger sample size, with diverse racial composition, and accounting for other confounding variables that may also contribute to the normal variation of olfactory sensitivities, such as the sensorineural factors or the potential effect of the nasal cycle. To fully capture the effect of the nasal cycle, a time series of CT scans or, at least, prenasal decongestant versus postnasal decongestant CT scans would be needed, which would require new experimental protocols in the future. The current results only reflect a snapshot among a cohort of subjects who might be in different phases of the nasal cycle. In our data analysis, the bilateral nasal index value was assigned to both sides for each nose. This is imperfect, but at least, offers some way to compare the nasal anatomical variations with the rest of the unilateral variables. With further validation, the newly defined objective parameter, notch index, may serve better to quantify the nasal anatomical variations for the future studies.

### Conclusion

This study integrates computational simulations and experimental measurements to reveal a potential impact of normal variation in nasal structure and aerodynamics on normative variations in olfactory sensitivity.

### Funding

This work was supported by the National Institutes of Health [NIH NIDCD R01 DC013626 to K.Z.].

### Acknowledgments

The authors would like to thank Kara Blacker, Yuehao Luo for assistance with data collection, and Dr Peter W Scherer for scientific discussions.

### References

- Clement PA. 1984. Committee report on standardization of rhinomanometry. *Rhinology*. 22:151–155.
- Damm M, Vent J, Schmidt M, Theissen P, Eckel HE, Lötsch J, Hummel T. 2002. Intranasal volume and olfactory function. *Chem Senses*. 27:831–839.

- DeMaria S, Berke AP, Van Name E, Heravian A, Ferreira T, Ngai J. 2013. Role of a ubiquitously expressed receptor in the vertebrate olfactory system. *J Neurosci.* 33:15235–15247.
- Doddi NM, Eccles R. 2011. The relationship between nasal index and nasal airway resistance, and response to a topical decongestant. *Rhinology.* 49:583–586.
- Hahn I, Scherer PW, Mozell MM. 1993. Velocity profiles measured for airflow through a large-scale model of the human nasal cavity. *J Appl Physiol (1985).* 75:2273–2287.
- Hornung DE, Youngentob SL, Mozell MM. 1987. Olfactory mucosa/air partitioning of odorants. *Brain Res.* 413:147–154.
- Ignatieva EV, Levitsky VG, Yudin NS, Moshkin MP, Kolchanov NA. 2014. Genetic basis of olfactory cognition: extremely high level of DNA sequence polymorphism in promoter regions of the human olfactory receptor genes revealed using the 1000 Genomes Project dataset. *Front Psychol.* 5:247.
- Kelly JT, Prasad AK, Wexler AS. 2000. Detailed flow patterns in the nasal cavity. *J Appl Physiol (1985).* 89:323–337.
- Keyhani K, Scherer PW, Mozell MM. 1995. Numerical simulation of airflow in the human nasal cavity. *J Biomech Eng.* 117:429–441.
- Keyhani K, Scherer PW, Mozell MM. 1997. A numerical model of nasal odorant transport for the analysis of human olfaction. *J Theor Biol.* 186:279–301.
- Lee TS, Goyal P, Li C, Zhao K. 2018. Computational fluid dynamics to evaluate the effectiveness of inferior turbinate reduction techniques to improve nasal airflow. *JAMA Facial Plast Surg.* doi:10.1001/jamafacial.2017.2296.
- Leong SC, Chen XB, Lee HP, Wang DY. 2010. A review of the implications of computational fluid dynamic studies on nasal airflow and physiology. *Rhinology.* 48:139–145.
- Leong SC, Eccles R. 2009. A systematic review of the nasal index and the significance of the shape and size of the nose in rhinology. *Clin Otolaryngol.* 34:191–198.
- Leopold DA. 1988. The relationship between nasal anatomy and human olfaction. *Laryngoscope.* 98:1232–1238.
- Li C, Farag A, Maza G, McGhee S, Ciccone M, Deshpande B, Pribitkin E, Otto B, Zhao K. 2018. Investigation of the abnormal nasal aerodynamics and trigeminal functions among empty nose syndrome patients. *Int. Forum Allergy Rhinol.* 8: 444–452.
- Li C, Farag AA, Leach J, Deshpande B, Jacobowitz A, Kim K, Otto BA, Zhao K. 2017. Computational fluid dynamics and trigeminal sensory examinations of empty nose syndrome patients. *Laryngoscope.* 127:E176–E184.
- Li C, Jiang J, Dong H, Zhao K. 2017. Computational modeling and validation of human nasal airflow under various breathing conditions. *J Biomech.* 64:59–68.
- Mainland JD, Keller A, Li YR, Zhou T, Trimmer C, Snyder LL, Moberly AH, Adipietro KA, Liu WL, Zhuang H, et al. 2014. The missense of smell: functional variability in the human odorant receptor repertoire. *Nat Neurosci.* 17:114–120.
- Menashe I, Man O, Lancet D, Gilad Y. 2003. Different noses for different people. *Nat Genet.* 34:143–144.
- Otto BA, Li C, Farag AA, Bush B, Krebs JP, Hutcheson RD, Kim K, Deshpande B, Zhao K. 2017. Computational fluid dynamics evaluation of posterior septectomy as a viable treatment option for large septal perforations. *Int Forum Allergy Rhinol.* 7:718–725.
- Pribitkin E, Rosenthal MD, Cowart BJ. 2003. Prevalence and causes of severe taste loss in a chemosensory clinic population. *Ann Otol Rhinol Laryngol.* 112:971–978.
- Ramprasad VH, Frank-Ito DO. 2016. A computational analysis of nasal vestibule morphologic variabilities on nasal function. *J Biomech.* 49:450–457.
- Scott JW, Sherrill L, Jiang J, Zhao K. 2014. Tuning to odor solubility and sorption pattern in olfactory epithelial responses. *J Neurosci.* 34:2025–2036.
- Shen J, Hur K, Li C, Zhao K, Leopold D, Wrobel B. 2017. Erratum: Determinants and Evaluation of Nasal Airflow Perception. *Facial Plast Surg.* 33:553–554.
- Shen J, Hur K, Zhao K, Leopold DA, Wrobel BB. 2017. Determinants and evaluation of nasal airflow perception. *Facial Plast Surg.* 33:372–377.
- Sobel N, Prabhakaran V, Hartley CA, Desmond JE, Glover GH, Sullivan EV, Gabrieli JD. 1999. Blind smell: brain activation induced by an undetected air-borne chemical. *Brain.* 122 (Pt 2):209–217.
- Spitze K. 1993. Population structure in *Daphnia obtusa*: quantitative genetic and allozymic variation. *Genetics.* 135:367–374.
- Stuiver M. 1958. Biophysics of the sense of smell [dissertation]. Groningen, The Netherlands: Rijks University.
- Subramaniam RP, Richardson RB, Morgan KT, Kimbell JS, Guilmette RA. 1998. Computational fluid dynamics simulations of inspiratory airflow in the human nose and nasopharynx. *Inhal Toxicol.* 10:91–120.
- Swift DL, Proctor DF. 1977. Access of air to the respiratory tract. In: Brain JD, Proctor DF, Reid LM, editors. Respiratory defense mechanisms. New York: Marcel Dekker pp. 63–93.
- Thomson A, Buxton LD. 1923. Man's nasal index in relation to certain climatic conditions. *J Anthropol Inst Great Britain and Ireland.* 53:92–122.
- Wetherill GB, Levitt H. 1965. Sequential estimation of points on a psychometric function. *Br J Math Stat Psychol.* 18:1–10.
- Whitlock MC, Guillaume F. 2009. Testing for spatially divergent selection: comparing QST to FST. *Genetics.* 183:1055–1063.
- Wilcox D. 2006. One-equation and two-equation Models. In: Wilcox DC, editor. *Turbulence Modeling for CFD.* 3rd ed. La Canada (CA): DCW Industries. p. 107–230.
- Zaidi AA, Mattern BC, Claes P, McEcoy B, Hughes C, Shriver MD. 2017. Investigating the case of human nose shape and climate adaptation. *PLoS Genet.* 13:e1006616.
- Zhao K, Dalton P. 2007. The way the wind blows: implications of modeling nasal airflow. *Curr Allergy Asthma Rep.* 7:117–125.
- Zhao K, Dalton P, Yang GC, Scherer PW. 2006. Numerical modeling of turbulent and laminar airflow and odorant transport during sniffing in the human and rat nose. *Chem Senses.* 31:107–118.
- Zhao K, Jiang J. 2014. What is normal nasal airflow? A computational study of 22 healthy adults. *Int Forum Allergy Rhinol.* 4:435–446.
- Zhao K, Jiang J, Pribitkin EA, Dalton P, Rosen D, Lyman B, Yee KK, Rawson NE, Cowart BJ. 2014. Conductive olfactory losses in chronic rhinosinusitis? A computational fluid dynamics study of 29 patients. *Int Forum Allergy Rhinol.* 4:298–308.
- Zhao K, Pribitkin EA, Cowart BJ, Rosen D, Scherer PW, Dalton P. 2006. Numerical modeling of nasal obstruction and endoscopic surgical intervention: outcome to airflow and olfaction. *Am J Rhinol.* 20:308–316.
- Zhao K, Scherer PW, Hajiloo SA, Dalton P. 2004. Effect of anatomy on human nasal air flow and odorant transport patterns: implications for olfaction. *Chem Senses.* 29:365–379.